Skeletonization of Potential-Field and Seismic Images

Le Gao* and Igor Morozov, University of Saskatchewan, Saskatoon, Saskatchewan
le.gao@usask.ca

GeoConvention 2012:Vision

Summary

We apply skeletonization approach to geophysical data to recognize geologic structures and pick seismic horizons automatically. We formulate the technique to be explicitly applicable to all gridded geophysical data. The method consists in extracting multiple features of "wavelets" which may be single or double peaks or troughs characterized by amplitudes, widths, orientation angles, spatial dimensions, polarities, and other attributes. The wavelets are further connected based on similarities of these attributes to form the "skeleton" of the geophysical image. In addition, optional 2-D or 1-D filtering conducted during the identification process allows extracting parameters of background trends and reduce the adverse effects of low frequencies on skeletonization. Gravity, magnetic, and seismic data are used to illustrate the utility and effectiveness of the algorithm. The results show that the approach is useful for identifying structures in complex geophysical images and for automatic extraction of their attributes.

Introduction

Geophysical data are used to study the structure, composition, dynamic changes, and to provide reliable models of the Earth based on the principles of physics. Although the types of geophysical images, such as seismic, gravity, and magnetic maps, are variable, they also possess a number of common features. In two-dimensional (2-D) images, such features can often be expressed by using the amplitudes, widths, polarities, orientation angles and/or other attributes of some "anomalies", or "wavelets". Automatic identification of such spatially-connected wavelets and measurement of their parameters is the general objective of the pattern-recognition process called "skeletonization".

The geophysical skeletonization technique was developed initially for automatic event picking in reflection seismic data (Le and Nyland, 1990; Lu and Cheng, 1990; Li and Vasudevan, 1997; Li et al., 1997). In these approaches, pattern primitives (amplitudes, durations and polarities) were extracted from seismic traces and connected according to similar features to determine coherent events. Strong seismic events were used as a guide to track weaker events and find connections iteratively. These approaches were based on the binary consistency-checking (BCC) scheme by Cheng and Lu (1989). Eaton and Vasudevan (2004) extended this type of skeletonization to aeromagnetic data by introducing two-pass spatial processing and measuring strike directions, event linearities, amplitudes, and polarities.

Because they are derived from seismic processing, the existing geophysical skeletonization approaches are limited to near-zero mean wavelets. Even in reflection seismic records, a low-frequency background can thwart feature extraction and cause disruptions in the "skeleton". For example, because of a positive bias in amplitudes, the waveform in Figure 1 would only be identified as a single wavelet. However, it would definitely be better to recognize two positive peaks within this wavelet. Pre-filtering of the image prior to event detection could also be undesirable, as this could complicate processing and cause losing the information about the background trend. For potential-field data, the above issues become particularly important and complex. In addition, although skeletonization of gridded data in two passes in orthogonal directions (Eaton and Vasudevan, 2004) allows detecting features at arbitrary orientation, the sensitivity of this detection still remains azimuthally non-uniform.

In this paper, we propose a skeletonization technique specifically designed for 2-D gridded geophysical data. Seismic (pre- or post-stack) records are only considered as special cases of such grids, with specific treatment of the time dimension and also additional constraints and attributes. While achieving the same general goals of quantitative recognition of linear features in gridded images, the present approach differs from the existing ones by: 1) feature detection performed isotropically, at a continuous range of angles, 2) use of some new features, such as orientation angles and background-trend level, to meet the complexity of the data, and 3) use of a more flexible event detection scheme instead of the BCC.

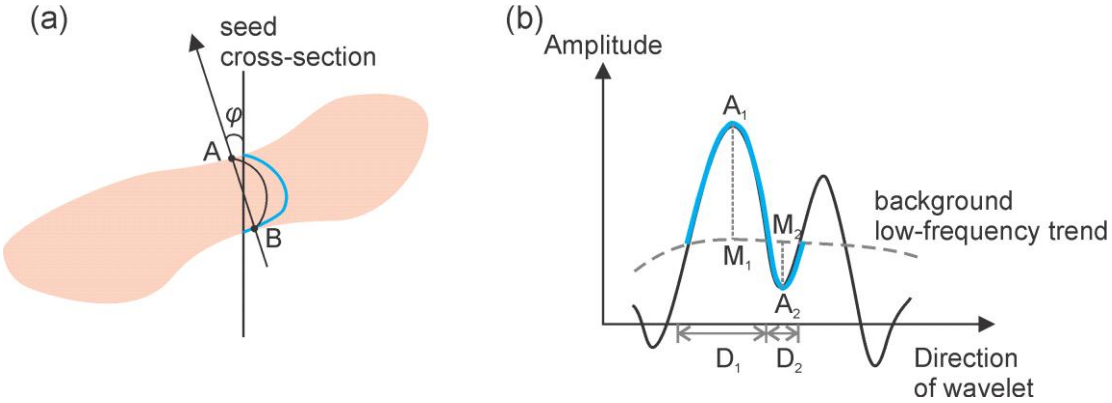

Figure 1: Wavelet extraction: (a) Extraction of an anomaly (pink) from a seed cross-section. AB is the minimal cross-sectional size;

(b) Identification of wavelet attributes. Blue line is the extracted wavelet. A_1 and A_2 is peak and trough amplitudes, respectively; M_1 and M_2 are the background amplitudes; D_1 and D_2 are the widths of the peak and trough.

The approach is implemented as part of a broader processing and interpretation environment, which allows handling, filtering in various ways, and displays of 2-D gridded, as well as of seismic and well-log data (Chubak and Morozov, 2006). This environment also offers a unique capability of using large volumes of potential-field data in the traditional, serial, seismic-processing type processing. As shown in data examples below, this results in a flexible algorithm capable of working with potential-field as well as pre- and post-stack seismic data.

Method

Similarly to the previous approaches (e.g., Eaton and Vasudevan, 2004), skeletonization is achieved in two principal steps:1) identification of elementary “wavelets” in the gridded images, and 2) connection of these wavelets to form the “skeleton” of the image. In the potential-field case, the skeleton comprises the “lineaments” detected in the image, and in seismic case, it can be interpreted as a set of “horizons”.

1) **Wavelet Detection and Feature Extraction.**

Starting from a grid of “seed” vertical or horizontal cross-sections, wavelets in the 2-D grid are identified as combinations of one or two amplitude deviations from the background trend level. We refer to these deviations as “humps” (Figure 1). Humps are first searched within the cross-section line, and then their orientation azimuths are determined by minimizing the cross-sectional sizes (AB in Figure 1a). With the new feature of subtracting the slow-varying trend, the humps are identified even on top of a slowly-varying amplitude background (Figure 1b). Once the wavelets are isolated, their polarities (directions) are determined by comparing the two humps within them (as by Eaton and Vasudevan, 2004) or also by the comparing the amplitudes of adjacent wavelets. “Undefined” values of polarities are also allowed where they cannot be determined consistently.

For subsequent pattern analysis, the wavelets are determined by peak or trough amplitudes (A_1 and A_2), widths (D_1 and D_2), orientation angles (φ), background levels and polarities P, Figure 1b). These parameters represent the feature sets:

$$f = \left(A_1, A_2, D_1, D_2, M_1, M_2, \varphi, P\right) . \quad (1)$$

2) Wavelet connections

After all wavelet features are determined, they are spatially connected to form the skeleton. This process is started from either: 1) wavelets manually picked by the user or 2) the strongest amplitudes. First, each selected wavelet is connected to several adjacent wavelets according to the lowest connection costs. The cost function is designed to evaluate the similarity of two wavelets. For example, for humps *A* and *B*, the cost function is (Figure 2),

$$\text{Cost}(A,B) = \sum_i w_i \left| \mathbf{f}_i^A(\mathbf{r}^A) - \mathbf{f}_i^B(\mathbf{r}^B) \right|, \quad (2)$$

where $\mathbf{r}^A$ and $\mathbf{r}^B$ are the spatial coordinates, $\mathbf{f}^A$ and $\mathbf{f}^B$ are the corresponding feature vectors (1), and w_i are some empirically-determined weights.

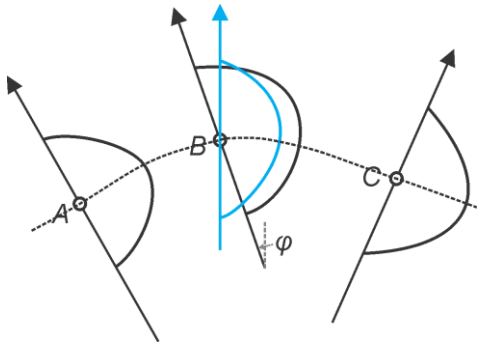

Figure 2: Horizon connection.

Wavelet *A* and *C* are interpolated at the location of *B* (blue) and cross-correlated with wavelet *B*. Dotted line is the proposed connections tested for optimality.

Among all pairs of potential connections, optimal triplets are further found. For example, for wavelet B in Figure 2, several candidates for adjacent connections *A* and *C* are considered based on the orientation angle, φ. Among these candidates, the optimal pair is found by minimizing the following cost function:

$$\text{Cost}(A,B) + \text{Cost}(B,C) + \left| \text{interp}(B) - \frac{\text{interp}(A) + \text{interp}(C)}{2} \right|, \quad (3)$$

where interp(*B*) (blue line in Figure 2) is the feature set interpolated at location *B* by using wavelets *A* and *C*. and their mutual cost functions, *Cost(A,B)* and *Cost(B,C).* Note that this triplet connection scheme does not use the somewhat arbitrary Euclidian distance and area-of-triangle principles used by Li and Vasudevan (1997) but measures the similarity of wavelets directly by their zero-lag cross-correlation (Figure 2).

Examples

Several examples of potential-field and seismic data are used to illustrate the usefulness of our algorithm. In Figure 3 and 4 are magnetic and gravity examples using regional gridded datasets for Southern Saskatchewan and Southwestern Manitoba obtained from Natural Resources Canada. In these Figures, note the dominant linear event trends, which are SW-NE in the northern parts of the images and NW-SE in the southern areas. The “skeleton” of the image also includes the amplitudes of positive anomalies, which are indicated by the sizes of circles plotted in these Figures.

Figure 5a shows a small portion of the seismic stacked section from Weyburn Oil Field. In Figure 5, the corresponding skeleton image is given, with coloured circles indicating the peak and trough amplitudes. These amplitudes were extracted on top of a background trend, which was identified by smoothing using a 30-ms sliding window. Note that the connections show the correct trends despite the slow-varying amplitudes present between 1060–1090 ms in the seismic records (Figure 5a).

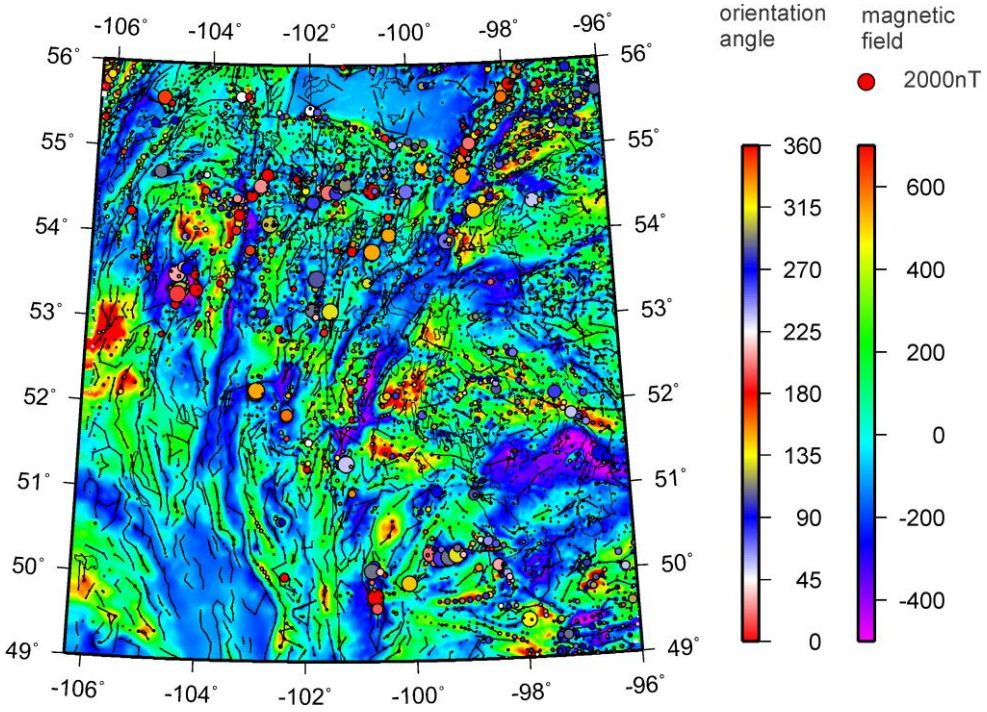

Figure 3: Aeromagnetic map of southern Saskatchewan and SW Manitoba.

The circles indicate major features and the lines are picked linear anomalies. Colours of the circles correspond to orientations of the anomalies, relative to the North-South direction (see palette).

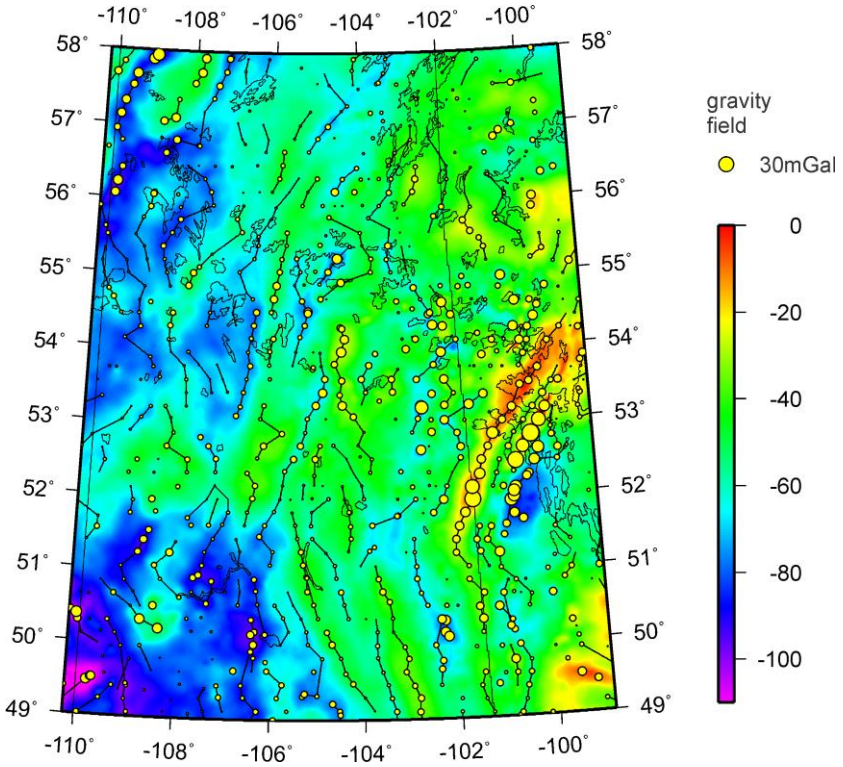

Figure 4: Regional gravity data example. The lines are feature connections. Circle sizes indicate the amplitudes of the anomalies. Yellow circles indicate positive-polarity and the purple indicates the negative polarity.

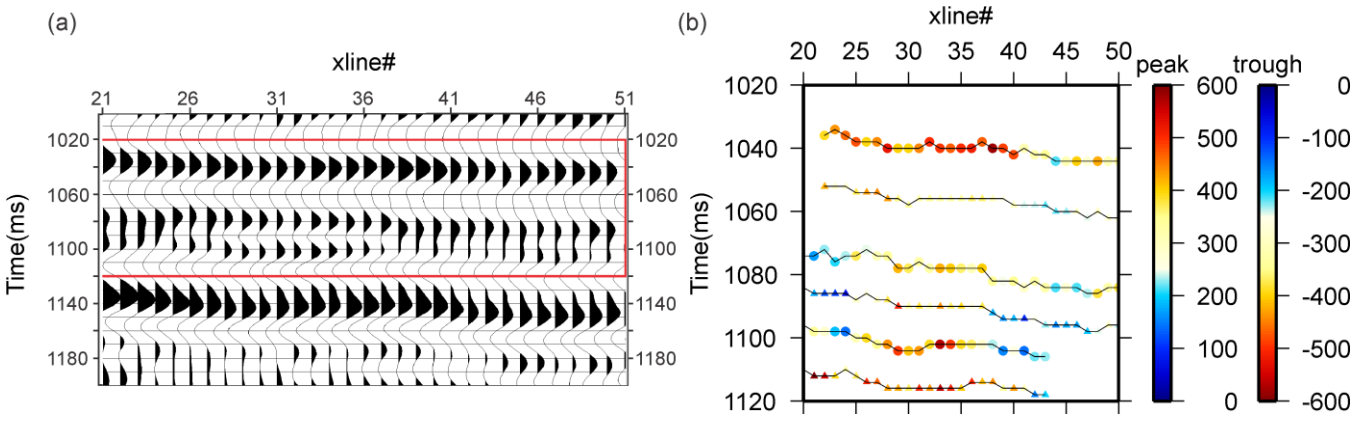

Figure 5: Seismic data example: a) stacked section; b) is the skeleton image from the area marked by the red rectangle (1020ms~1120ms) in plot a), colour bars show amplitudes of peaks and troughs.

Conclusions

The geophysical skeletonization proposed in this paper is effective and useful for pattern recognition in potential-field and seismic images. The process of skeletonization could identify and characterize the anomalies by correlating the adjacent wavelets. Compared with previous methods, our algorithm is more general, isotropic in feature detection, and applicable to arbitrary gridded geophysical data. The algorithm is also integrated in a powerful seismic/potential-field data processing system. With the new options for background-trend extraction, it provides more stable identification of lineaments and horizons. The skeleton image represents a convenient and quantitative tool for delineating geological structures in the maps or for auto-picking horizons in seismic images. The wavelets obtained by scanning gridded data along the orientation angles facilitate structure detection and its quantitative characterization. The results of both potential-field and seismic data illustrate that the skeletonization could aid in the interpretation for complex structures. Some future applications to advanced geophysical attributes, such as seismic amplitude versus offset, are being developed.

Acknowledgements

This work was supported by Saskatchewan Energy and Resources and in part by Phase II of IEA GHG Weyburn CO_2 Storage and Monitoring Project.

References

Cheng, Y. C., and Lu, S. Y., 1989, The binary consistency checking scheme and its applications to seismic horizon detection: IEEE, Trans. Pattern Analysis, **11**,439-447.

Chubak, G., Morozov, I.B., 2006, Integrated software framework for processing of geophysical data. Computers & Geosciences **32(6)**, 767–775.

Eaton, D., and Vasudevan, K., 2004, Skeletonization of aeromagetic data: Geophysics, **69**, 478-488.

Le, L. H. T., and Nyland, E., 1990, Pattern analysis of seismic records: Geophysics, **55**, 20-28.

Li, Q., and Vasudevan, K., and Cook, F. A., 1997, Seismic skeletonization: A new approach to interpretation of seismic reflection data: Journal of Geophysical Research, **102**, 8427-8445.

Lu, S. Y., and Cheng, Y. C., 1990, An iterative approach to seismic skeletonization: Geophysics, **55**, 1312-1320.